

Simulation of a 1 Dimensional N Particle System in Thermodynamic Equilibrium

Kurran Singh Bharaj

December 18, 2017

Contents

1	Introduction	2
2	Background	3
2.1	Information Theory	3
2.2	Landauer's Principle	3
2.3	Maxwell's Demon	3
2.4	Quantum Thermodynamics	4
2.5	Quantum Szilard Engine	4
3	Single particle in a box	6
3.1	Classical density of states	6
3.2	Thermodynamic entropy	6
3.3	Quantum statistics	7
3.4	Evaluation of the Fermi-Dirac chemical potential	8
3.5	Energy of a fermi gas	9
3.6	Entropy of a fermi gas	10
4	Microstate Analysis	11
4.1	Stirling Approximation Error	12
4.2	N Identical Particles in an Infinite Well	12
4.3	Enumerating over N-Particle Basis States	15
4.4	Maximum Temperature for an N level system	17
4.5	Recovering Fermi-Dirac Statistics	20
5	Calculating Thermodynamic Variables	22
6	Quantum Szilard Engine	24
7	Conclusions	29
8	References	30

1 Introduction

The first part of this project introduces standard quantum statistics. Quantum statistics are used to analyse a 1 Dimensional infinite well system. Fermi-Dirac statistics are used to derive the low temperature behaviour of the system and the system is analysed explicitly. The limitations of this analysis are then explained. To overcome the limitations the system is modelled as a fully quantum system with N particles in thermal equilibrium. I have calculated the density matrix that describes the system, and this has been used to calculate various thermodynamic properties of the system which included the partition function. Using the partition function I have gone on to suggest an approach to verify Landauer's principle by treating the quantum system as a Szilard Engine. The system is well defined and should make it easier to unambiguously demonstrate the thermodynamic entropy cost.

2 Background

2.1 Information Theory

In 1948 Claude Shannon [1] introduced the idea of information entropy when transmitting messages. Information entropy refers to the lower limit of information that can be encoded in an n -bit message without errors. This is dependant on the probability of each bit occuring next in the message. Shannon entropy provides a lower bound for the compression that can be achieved by the data representation (coding) compression step. Shannon defined the entropy H of a message with bits x_i and b is the base of the logarithm (a value of 2 when used with information theory).

$$H(x) = - \sum_{i=1}^n P(x_i) \log_b P(x_i) \quad (1)$$

2.2 Landauer's Principle

Landauer's principle was first proposed by Rolf Landauer in 1961. [2] It states that the erasure of n bits of information must always require a minimum energy cost of thermodynamic entropy as shown

$$k_B T \ln 2 \quad (2)$$

(2) is the minimum energy dissipated (approximately 0.0172 eV at room temperature). k_B is the Boltzmann constant and T is the temperature. This increase in entropy occurs when there has been an irreversible computational operation; this is a change in the system. This can be either through compression of a message or through logical computational operations such as "AND" or "OR". In both cases the erasure of information results in an energy cost of $k_B T \ln 2$ per bit of information. [3] The principal was later expanded upon by Bennet who wrote about the benefits of reversible computing.[4] To this day, the erasure principle is still regarded as highly controversial and has been disputed several times. [5][6][7] Ultimately it is argued that the principal has not been properly verified, and any such verifications such as [8] [9] point out flaws in the thermodynamic system used.

2.3 Maxwell's Demon

The principle is perhaps most famous for offering a solution to Maxwell's demon which began as a thought experiment first mentioned in 1867. The second law of thermodynamics states that the entropy of any isolated system always increases. In the thought experiment, a closed system is imagined with a door in the middle. A 'demon' controls the door; opening and closing it so fast such that gas molecules with more kinetic energy end up on one side as shown in Figure 1. Thus the second law of thermodynamics is violated; the entropy of the system is lowered (one side heats up as the other cools down). Landauer's theory offered a counter to this. The resolution of this paradoxical situation is that the demon

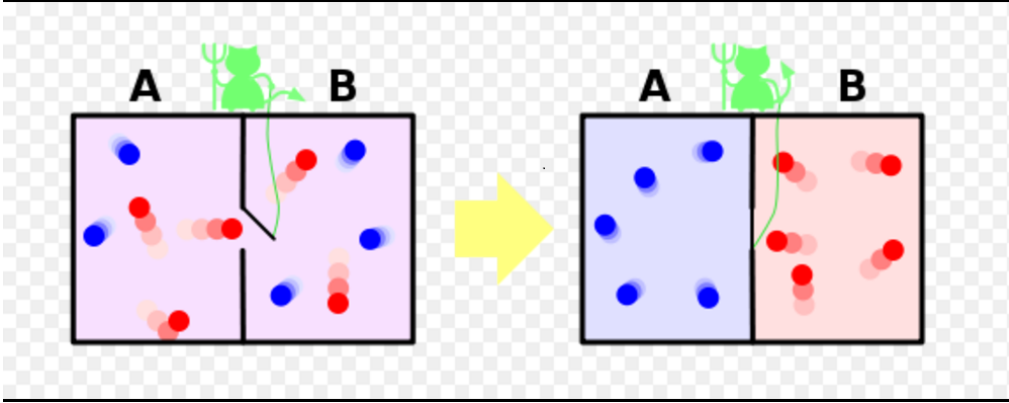


Figure 1: Maxwell's demon

needs to gather information about individual gas particles in order to choose which ones to let through and which ones to not. In choosing which molecules to select after each operation, the demon would need to erase ('forget') the information it used; this information is converted to heat, incurring a hidden entropy cost in the erasure of information. This is greater than the entropy lost by the demon thus preserving the second law of thermodynamics. This insight; that information erasure leads to heat generation has led to a long standing connection between physics and information theory. [10]

2.4 Quantum Thermodynamics

For non equilibrium states, quantum thermodynamic entropy is the same as the von Neumann entropy for equilibrium states.[11]

$$S(\rho) := -\text{tr}(\rho \ln \rho) \quad (3)$$

ρ is the density operator, and can be expanded as follows. H is the Hamiltonian of the system and $\beta = \frac{1}{k_B T}$

$$\rho = \frac{e^{-\beta H}}{\text{Tr}(e^{-\beta H})} \quad (4)$$

$$\rho = \frac{e^{-\beta H + vN}}{\text{Tr}(e^{-\beta H + vN})} \quad (5)$$

$$\rho = \frac{e^{-\beta H + \sum_{i=1}^n v_i N_i}}{\text{Tr}(e^{-\beta H + \sum_{i=1}^n v_i N_i})} \quad (6)$$

2.5 Quantum Szilard Engine

The Szilard engine is a kind of heat engine that serves as natural extension to Maxwell's demon.[12] A simple version of the Szilard engine consists of a single

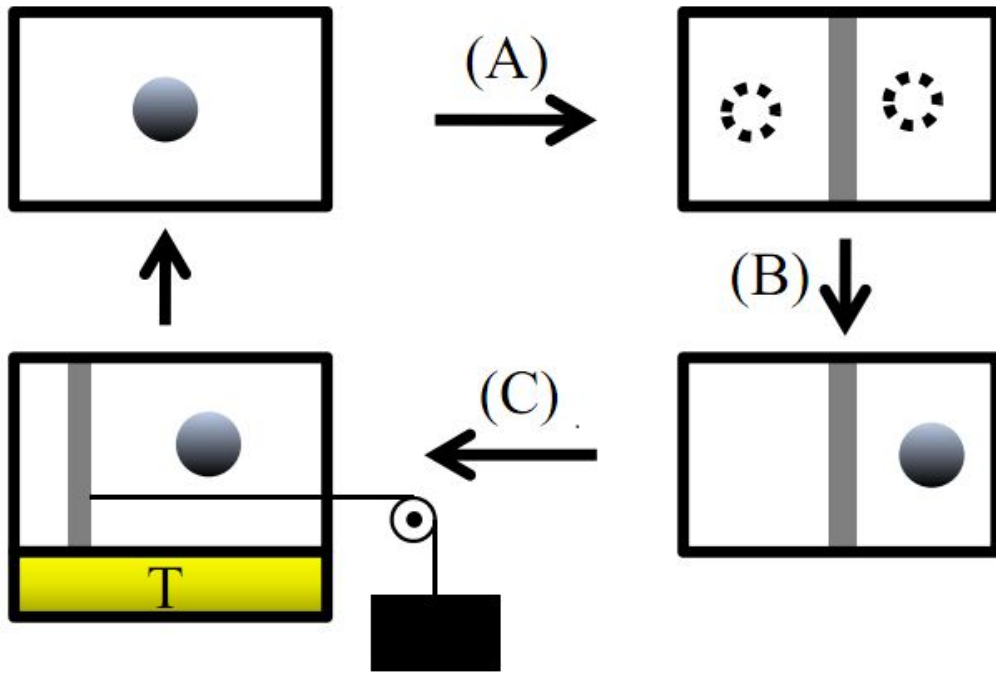


Figure 2: Szilard Engine

particle in a box that is operated by a 'demon'. The heat engine operates in a cyclical process. First there is an insertion of a partition to split the box into separate parts. The particle's position at this point is currently not known or influenced (if placed in the middle it has an equal probability of being on either side). Next comes the act of measuring which side of the partition the particle resides. The demon records this information and an external load (such as a weighted pulley) is attached to the partition. The partition is free to move and act as a piston; the piston is allowed to move back into equilibrium whilst in thermal contact with a heat reservoir. After the partition is removed the system is returned to its original state with no net increase in entropy and having done useful work extracting heat from its surroundings. This cycle violates the second law of thermodynamics, Landauer's principle once again serves to preserve the second law. [13]

3 Single particle in a box

We start our analysis using the simple quantum mechanical particle in a box. Consider a particle in a one-dimensional box of length L . Inside the box the potential is zero and outside the box the potential is infinite. This precludes a particle from existing outside the box. Both quantum mechanics and statistical mechanics can start from this same, simple model. Within the box the particle is free to move. Elementary wave theory shows that a particle's energy is quantised. The particles exist in discrete energy eigenstates of energy ϵ given by

$$\epsilon(n) = \frac{\pi^2 \hbar^2 n^2}{2mL^2} \quad (7)$$

Each quantum state is uniquely defined by the quantum number n .

3.1 Classical density of states

In the classical regime the confining volume (or length for one dimension) is macroscopically large. From equation 7 we see that for large L the energy between adjacent states reduces. In classical statistical mechanics the volume is assumed to be large. In this approximation the discrete quantum states $\epsilon(n)$ are approximated to a continuum of states. The number of states up to energy $\epsilon(n)$ is given by

$$N(\epsilon) = \frac{L}{\hbar\pi} (2m\epsilon)^{\frac{1}{2}} \quad (8)$$

The density of states $g(\epsilon)$ is given by

$$g(\epsilon) = \frac{dN(\epsilon)}{d\epsilon} \quad (9)$$

and from 8 this gives the density of states per unit length as

$$g(\epsilon) = \frac{1}{\hbar\pi} \sqrt{\frac{m}{2\epsilon}}. \quad (10)$$

3.2 Thermodynamic entropy

The single particle partition function is given by

$$\begin{aligned} z &= \int_0^\infty g(\epsilon) e^{-\epsilon/k_B T} d\epsilon \\ &= \frac{1}{\hbar\pi} \sqrt{\frac{m}{2}} \int_0^\infty \epsilon^{-1/2} e^{-\epsilon/k_B T} d\epsilon \\ &= L \left(\frac{2\pi m k_B T}{h^2} \right)^{1/2} \end{aligned}$$

where the final integral is a gamma function. For N indistinguishable particles the partition function Z is given by

$$Z = \frac{1}{N!} z^N.$$

Using Stirling's approximation to evaluating the logarithm of Z we get

$$\ln Z = -N \ln N + N + N \ln z = N \ln \left[L \left(\frac{2\pi m k_B T}{h^2} \right)^{1/2} \frac{1}{N} \right]$$

Helmholtz free energy is given by

$$F = -kT \ln Z = -NkT \ln \left[L \left(\frac{2\pi m k_B T}{h^2} \right)^{1/2} \frac{1}{N} \right]$$

the total internal energy is given by

$$E = kT^2 \frac{\partial \ln Z}{\partial T} \Big|_L = NkT^2 \frac{d \ln T^{3/2}}{dT} = \frac{3}{2} NkT$$

and entropy is

$$S = -\frac{\partial F}{\partial T} \Big|_V = Nk \ln \left[\left(\frac{mkT}{2\pi \hbar^2} \right)^{3/2} \frac{V e^{5/2}}{N} \right]$$

This is clearly a physically incorrect result. As T tends to zero the entropy tends to $-\infty$ in violation of the third law of thermodynamics. The classical result is therefore insufficient to analyse low temperature behaviour. The reason for the breakdown at low temperatures is because classical physics assumes that available states are plentiful and particles never compete for occupancy. In classical physics the particles do not interact.

3.3 Quantum statistics

In the following discussion the particles under consideration are fermions. Fermions obey the Pauli Exclusion principle, i.e. no two particles may occupy the same quantum state. This principle dictates the low temperature behaviour of fermions. As the temperature tends to zero, particles preferentially occupy the lowest energy states. At zero temperature the particles 'condense' into the lowest possible energy states. Pauli exclusion alone prevents the particles from occupying the lowest state at the same time. These properties are modelled by the Fermi-Dirac distribution

$$\bar{n}(\epsilon) = \frac{1}{\exp\left(\frac{\epsilon - \mu}{kT}\right) + 1} \quad (11)$$

where $\bar{n}(\epsilon)$ is the mean occupancy of states with energy ϵ and μ is chemical potential. The mean occupancy $\bar{n}(\epsilon)$ describes the probability of measuring a particle in a state with energy ϵ . Note that chemical potential μ is the energy when $\bar{n}(\epsilon) = \frac{1}{2}$. Although not stated explicitly in equation 11 the chemical potential is a function of temperature and the total number of particles in the system. To evaluate the chemical potential consider the system at $T = 0$. At $T = 0$ the distribution is just a box function. When $T = 0$ the chemical potential is called the Fermi Energy. For $\epsilon < \epsilon_F$ the energy state will definitely be measured

to be occupied. For $\epsilon > \epsilon_F$ the energy state will definitely be measured to be unoccupied.

In general the total number of particles N in a system is given by

$$N = \int_0^\infty \alpha \bar{n}(\epsilon) g(\epsilon) d\epsilon \quad (12)$$

where α is the degeneracy of each energy state and $g(\epsilon)$ is density of states. In the low temperature limit $\bar{n}(\epsilon)$ becomes a box function with transition at $\epsilon = \epsilon_F$. So at $T = 0$ equation 12 becomes

$$N = \int_0^{\epsilon_F} \alpha g(\epsilon) d\epsilon.$$

For spin- $\frac{1}{2}$ fermions $\alpha = 2$. We use the expression for the density of states $g(\epsilon)$ from equation 10 in the previous section which gives

$$\begin{aligned} N &= \frac{L}{\pi \hbar} \sqrt{m/2} \int_0^{\epsilon_F} \epsilon^{-1/2} d\epsilon \\ &= \frac{L \sqrt{4m}}{\pi \hbar} (\sqrt{\epsilon_F}) \end{aligned}$$

which after rearranging gives

$$\epsilon_F = \left(\frac{\pi \hbar N}{L} \right)^2 \frac{1}{4m}. \quad (13)$$

In a similar fashion the total energy of the system is given by

$$\begin{aligned} E &= \int_0^{\epsilon_F} \alpha g(\epsilon) \epsilon d\epsilon \\ &= \frac{\sqrt{4m}}{3\pi \hbar} \epsilon_F^{3/2} \end{aligned}$$

and from these results total energy E and total particle count N , at $T = 0$, are related by

$$E = \frac{1}{3} N \epsilon_F \quad (14)$$

3.4 Evaluation of the Fermi-Dirac chemical potential

To extend the analysis of the Fermi-Dirac distribution to $T > 0$ we need to determine $\mu(T)$. To do this we can start with the expression in equation 12 and substitute for α , $\bar{n}(\epsilon)$ and $g(\epsilon)$. This gives

$$N = \frac{L}{\pi \hbar} \sqrt{m/2} \int_0^\infty \frac{\epsilon^{1/2}}{e^{(\epsilon-\mu)/kT} + 1} d\epsilon$$

and substituting for N we get

$$\frac{1}{3} \epsilon_F^{1/2} = \int_0^\infty \frac{\epsilon^{1/2}}{e^{(\epsilon-\mu)/kT} + 1} d\epsilon. \quad (15)$$

This equation defines the chemical potential μ for arbitrary T . It cannot be evaluated easily by analysis and must be done numerically. To make this task amenable to a numerical methods define the dimensionless quantities $\tilde{\mu}$ and \tilde{T}

$$\tilde{\mu} = \frac{\mu}{\epsilon_F}$$

$$\tilde{T} = \frac{k_B T}{\epsilon_F}.$$

We further make a change of variable in the integral of $\epsilon \rightarrow x\epsilon_F$ which gives

$$\frac{1}{3} = \int_0^\infty \frac{x^{\frac{1}{2}}}{e^{(x-\tilde{\mu})/\tilde{T}} + 1} dx. \quad (16)$$

This has been solved numerically and a graph of $\tilde{\mu}$ versus \tilde{T} is shown in figure 3.

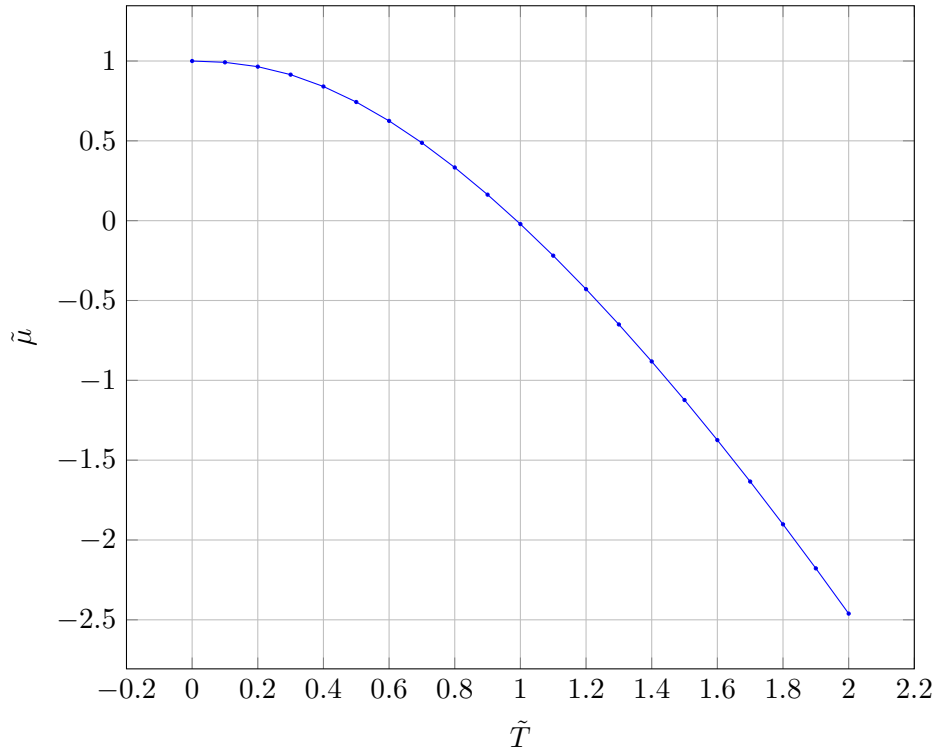


Figure 3: Reduced chemical potential versus reduced temperature.

3.5 Energy of a fermi gas

With full knowledge of the behaviour of $\mu(T)$ we can calculate macroscopic quantities from the quantum statistics. The total energy is a good example of macroscopic quantity that can be measured. The formula for the total energy

of a system is given in

$$U = \int_0^\infty \bar{n} \alpha g(\epsilon) \epsilon d\epsilon$$

which gives

$$U = \frac{L}{\pi \hbar} \sqrt{m/2}^{\frac{2}{3}} \epsilon_F^{\frac{5}{2}} G(\tilde{T}) \quad (17)$$

where $G(\tilde{T})$ is the dimensionless function of \tilde{T} given by

$$G(\tilde{T}) = \int_0^\infty \frac{x^{\frac{1}{2}}}{e^{(x-\bar{\mu})/\tilde{T}} + 1} dx \quad (18)$$

. The function $G(\tilde{T})$ completely encapsulates the variation of entropy with temperature and is plotted in 4.

3.6 Entropy of a fermi gas

For a quantum system we want to use the following definition for entropy

$$S = k_B \ln W \quad (19)$$

where W is the number of ways the microstates can be arranged such that the macrostate remains the same. In our example the microstates describe how fermi particles occupy energy eigenstates of the system. Our system is the 'particle in box' and consists of many energy eigenstates of energy ϵ_i . For each energy ϵ_i there may be n_i states associated with it. Each state can be considered a single 'compartment' for fermion to occupy. Now let there be N_i particles in energy eigenstates of ϵ_i where $N_i \leq n_i$. Now the compartments can be rearranged $n!$ different ways. However the particles are indistinguishable so we have over counted by $N_i!$. Also the vacancies are indistinguishable which means we have further over counted by $(N_i - n_i)!$ configurations. So the total number of configurations within this small energy range is

$$W_i = \frac{n_i!}{N_i! (N_i - n_i)!} \quad (20)$$

The total number of different configurations is simply the product of microstate configurations W_i so

$$W = \prod_i W_i \quad (21)$$

We can substitute into 19 using 20 and 21 to give

$$\begin{aligned} S &= k_B \ln \prod_i W_i \\ &= k_B \sum_i \ln n_i! - \ln N_i! - \ln(n_i - N_i)! \\ &= k_B \sum_i n_i \ln n_i - N_i \ln N_i - n_i \ln(n_i - N_i) + N_i \ln(n_i - N_i) \end{aligned}$$

and identifying $p_i = \frac{N_i}{n_i}$ as the probability of occupying the i^{th} energy state this becomes

$$S = -k_B \sum_i n_i [p_i \ln p_i + (1 - p_i) \ln(1 - p_i)]. \quad (22)$$

This can be converted to a continuum of states as has been done before. This converts the summation over energy states to an integral over energy to give

$$S = -k_B \int_0^\infty g(\epsilon) [\bar{n} \ln \bar{n} + (1 - \bar{n}) \ln(1 - \bar{n})] d\epsilon \quad (23)$$

where $\bar{n}(\epsilon)$ is probability of occupation (given by Fermi-Dirac statistics) and $g(\epsilon)$ is the density of states.

At $T = 0$ the fermi gas becomes degenerate. The particles only have one state, i.e. completely occupying energy levels below ϵ_F and no occupation above ϵ_F . This is the only configuration, i.e. $W = 1$ and so entropy is zero as expected. At higher temperatures the energy states are occupied with some probability allowing different possible configurations.

Inspecting equation 23 it is clear that energy states where $\bar{n}(\epsilon)$ is 0 or 1 do not contribute to the integral. This is because entropy is a measurement of uncertainty. States that are guaranteed to be occupied or empty do not contribute to the entropy. To plot equation 23 we use the previous technique to make it an integral of a dimensionless quantity. Making the substitution $\epsilon \rightarrow x\epsilon_F$ and converting μ and T to the dimensionless forms $(\tilde{\mu}, \tilde{T})$

$$S = \frac{-k_B V}{2\pi^2 \hbar^3} (2m)^{\frac{2}{3}} \epsilon_F^{\frac{3}{2}} H(\tilde{T})$$

where $H(\tilde{T})$ is the dimensionless function of \tilde{T} given by

$$H(\tilde{T}) = \int_0^\infty x^{\frac{1}{2}} [n \ln n + (1 - n) \ln(1 - n)] dx \quad (24)$$

noting that $n = n(x)$. The $H(\tilde{T})$ completely encapsulates the variation of entropy with temperature and is plotted in 4.

4 Microstate Analysis

The previous section reviewed the results of quantum statistics. That analysis suffers from a couple of serious drawbacks.

- The size of the system is assumed to be sufficiently large that the discrete energy levels form a continuum.
- The number of particles under consideration is sufficiently large and Stirling's approximation is used.

To demonstrate decisively that Maxwell's Daemon and Landaur's Principle are real laws they should ideally be tested on the quantum length scale where they cannot be masked by anything else. Ideally we would like to test this physics in an environment where the energy of a system could be directly measured. This would require a low temperature environment and relatively few particles. This is precisely the system that will be modelled in the next section.

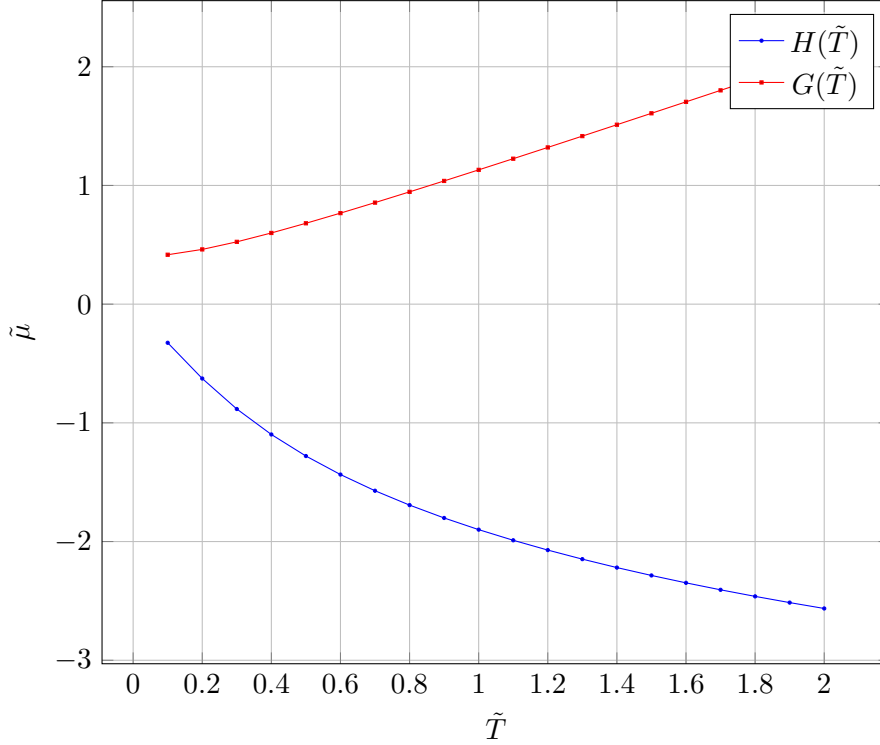


Figure 4: Variation of $H(\tilde{T})$ and $G(\tilde{T})$, temperature dependent parts of entropy and internal energy respectively.

4.1 Stirling Approximation Error

Quantum statistics makes heavy use of the Stirling approximation. This approximation is only valid for large N . For smaller values of N this approximation cannot be used in calculations as the error is too large as shown in Fig 5. When the Stirling approximation is used in conjunction with Fermi-Dirac statistics, only systems with a large number of particles should be analysed. For a low number of particles, an analysis should be performed from first principles. In the following section we begin to analyse such a system.

4.2 N Identical Particles in an Infinite Well

The system under consideration here is again the simple 1-dimensional infinite box containing N fermion particles. The energy levels available to the N Fermions are the energy levels of a single particle in a 1-dimensional well. The potential experienced by the particles is due to the confining potential. There is no interaction between the fermions. Their only interaction is via Pauli exclusion. A single particle wavefunction ψ_n with eigenenergy E_n

$$\hat{H}|\psi_n\rangle = E_n|\psi_n\rangle$$

where the value of the energy levels are given in .

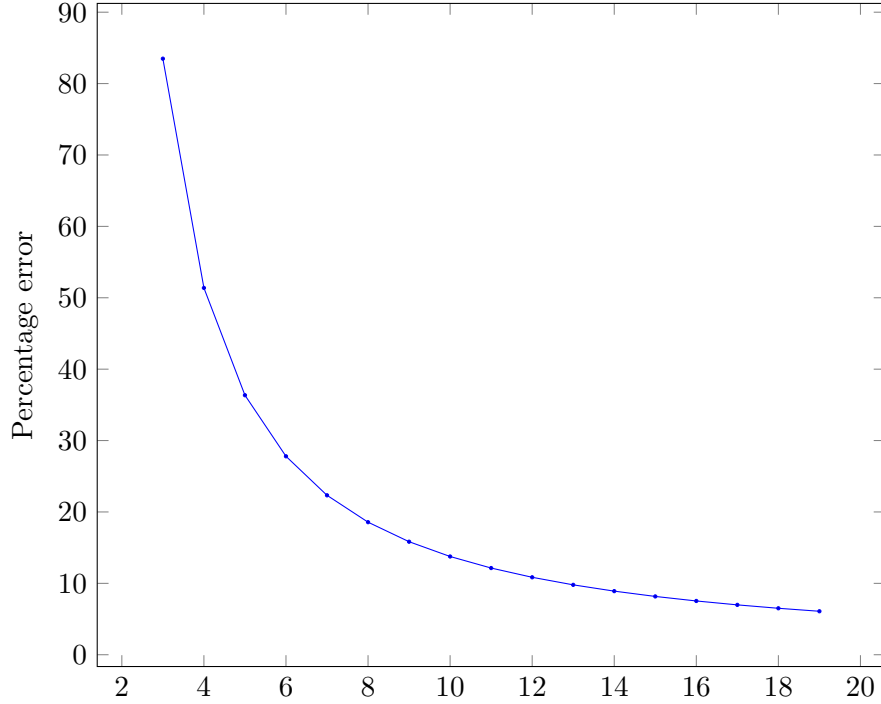


Figure 5: Percentage error of Stirling approximation versus N . For small values of N , the Stirling approximation is not suitable

For the multiparticle system we assume that the full N -particle state can be written as a product of N single particles states as in

$$|\Psi\rangle = |\psi_1\rangle|\psi_2\rangle\ldots|\psi_n\rangle \quad (25)$$

where each single particle state $|\psi_i\rangle$ describes the occupation a particular energy level n . The N -particle state is can only be written in this way because the individual particles have no mutual interaction terms. The Hamiltonian for the N -particle state is given by

$$\hat{H}|\psi_1\rangle|\psi_2\rangle\ldots|\psi_n\rangle = \left(\sum_{m=0}^N E_n\right) |\psi_1\rangle|\psi_2\rangle\ldots|\psi_n\rangle$$

The Hamiltonian of the system is simply the sum the of the energies of each particle in the system. These particles are in a perfectly good energy eigenstate and would remain so if not perturbed. In the canonical ensemble the disturbance arises from the continued thermalisation with a heat bath. The continued thermalisation with the surroundings means that systems state cannot be determined precisely. It is said to be in an impure state. The thermalisation will continually disturb the configuration of the system, redistributing the particles into different energy levels. The probability of measuring a particles in a configuration r with energy E_r is proportional to $\exp(-\beta E_r)$.

The impure state is best described by the density operator $\hat{\rho}$. The density operator can be written in an arbitrary basis as

$$\hat{\rho} = \frac{\exp\{-\beta\hat{H}\}}{\text{Tr}\left(\exp\{-\beta\hat{H}\}\right)} \quad (26)$$

and

$$\begin{aligned} \text{Tr}\left(\exp\{-\beta\hat{H}\}\right) &= \sum_s \langle \Psi_s | \exp\{-\beta\hat{H}\} | \Psi_s \rangle \\ &= \sum_s \langle \Psi_s | \exp\{-\beta E_s\} | \Psi_s \rangle \\ &= \sum_s \exp\{-\beta E_s\} \\ &= Z(T, V, N) \end{aligned}$$

In the energy representation $\hat{\rho}$ is diagonal,

$$\rho_{mn} = \rho_n \delta_{mn}$$

and the canonical density operator in the energy representation has diagonal elements given by

$$\rho_n = \frac{\exp\{-\beta E_n\}}{\sum_n \exp\{-\beta E_n\}} \quad (27)$$

where the partition function

$$Z = \sum_n \exp\{-\beta E_n\} \quad (28)$$

is used to normalise the elements of $\hat{\rho}$.

In the report the energy levels are assumed to support up to two fermions to model spin- $\frac{1}{2}$ particles. The energy levels indexed by n can increase with limit.

Any configuration of particles is possible. From a calculation of the density matrix all other observable quantities can be derived. For a some observable \hat{f} the expectation value is given by

$$\langle \hat{f} \rangle = \text{Tr}\left(\hat{\rho}\hat{f}\right) \quad (29)$$

Using this the internal energy of the system is given by

$$U = \langle \hat{H} \rangle = \frac{\text{Tr}\left(\exp\{-\beta\hat{H}\}\hat{H}\right)}{\text{Tr}\left(\exp\{-\beta\hat{H}\}\right)} \quad (30)$$

and entropy is

$$S = \langle -k \ln \hat{\rho} \rangle = -k \text{Tr}(\hat{\rho} \ln \hat{\rho}) \quad (31)$$

4.3 Enumerating over N-Particle Basis States

As discussed in the previous section the density matrix is an infinite matrix over the N -particle basis states. A single basis state describes the occupation of N particles over the different single-particle energy levels. The basis states may occupy any of the infinite single-particle energy levels available to them. Clearly we cannot consider all the basis states that may exist. Fortunately the probability of basis states existing decreases with energy. To calculate the diagonal terms of the density matrix, an algorithm was developed to methodically enumerate the N -particle basis states. If we consider only a subset m of the infinite energy levels for N identical particles to occupy where $2m \geq N$ then there are W distinct configurations where

$$W = \frac{(2m)!}{(2m - N)!N!}. \quad (32)$$

Figure 6 shows all the distinct configurations available in a 3-level system. A 3-level system, with a degeneracy per level of 2 can accommodate up to 6 particles. The configurations for the different number of particles are shown. Considering only 3 levels does not allow sufficiently high energy basis states to be considered. However we can build on the three level system and use it to extend to more levels. A lookup table for the known configurations within a 3 level system is created using the configurations in Figure 6.

For a many level system the levels are split into groups of three. The problem of distributing particles among individual energy levels involves first distributing them among groups of three energy levels. The problem is then reduced to enumerating combinations of particles amongs these three levels. The lowest energy configuration places particles in the lowest energy groups. The algorithm advances the configurations by promoting particles from one group to the adjacent group in a higher level. When particles are redistributed between groups all the micro configurations of the three level system (in the lookup table) are iterated over. The total number of states enumerated by the algorithm are counted. The correct functioning of the algorithm is confirmed by comparing the total number of states enumerated to the expected number of states using 32.

Figure 7 shows the frequency of configurations for a given energy for a 24 level system containing 8 particles. The fermi energy of the system is 60 and that is the point at which configurations start. The units of energy are $\frac{\pi^2 \hbar^2}{2mL^2}$, they correspond to the ground state energy level. The curve is roughly bell shaped because the most numerate configurations exist around the mean energy. Fewer configurations exist for higher energies where there are fewer levels. If it were not for the cap of 24 levels the number of configurations would rise exponentially with energy.

1 particle

```

-----  -----  -O-----
-----  -O-----  -----
-O-----  -----  -----
    1          2          3

```

2 particles

```

-----  -----  -----  -O-----  -----O-  -O--O-
-----  -O-----  -O--O-  -O-----  -----  -----
-O--O-  -O-----  -----  -----  -O-----  -----
    2          3          4          5          4          6

```

3 particles

```

-----  -----  -O-----  -O-----  -O--O-  -O-----  -O--O-
-O-----  -O--O-  -O-----  -O--O-  -O-----  -----  -----
-O--O-  -O-----  -O-----  -----  -----  -O--O-  -O-----
    4          5          6          7          8          5          7

```

4 particles

```

-----  -O-----  -O--O-  -O--O-  -O--O-  -O-----
-O--O-  -O-----  -----  -O-----  -O--O-  -O--O-
-O--O-  -O--O-  -O--O-  -O-----  -----  -O-----
    6          7          8          9         10          8

```

5 particles

```

-O-----  -O--O-  -O--O-
-O--O-  -O-----  -O--O-
-O--O-  -O--O-  -O-----
    9         10        11

```

6 particles

```

-O--O-
-O--O-
-O--O-
    12

```

Figure 6: Particle configurations for a 3-level system. Each level has a degeneracy of 2. All the distinct configurations the three level system are shown. The configurations are grouped by particle number.

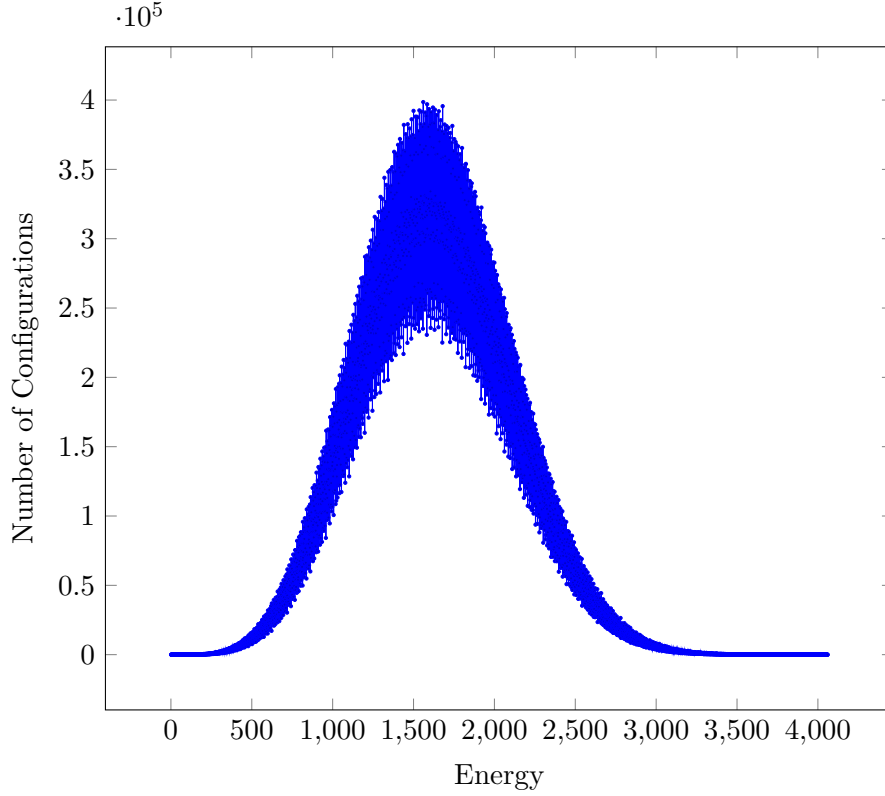


Figure 7: Number of configurations vs energy of configuration, energy is in units of $\frac{\pi^2 \hbar^2}{2mL^2}$

4.4 Maximum Temperature for an N level system

For an N -level system there will be several eigenstates enumerated each with their respective eigenenergies. Some eigenenergies will be undercounted by restricting the number of energy levels. There is a minimum energy below which we are guaranteed to count all the energy eigenstates. This energy corresponds to the lowest energy state where the $(N + 1)^{th}$ energy level is occupied. This lowest energy state is achieved by taking the state at $T = 0$ and promoting a single particle at the fermi level to the $(N + 1)^{th}$ energy level. The energy E_{max} of this state is given by

$$E_{max} = E_{T=0} - \epsilon_F + \epsilon(N + 1) \quad (33)$$

where $E_{T=0}$ is the energy of the degenerate state at $T = 0$, ϵ_F is the energy of the Fermi level and $\epsilon(N + 1)$ is the energy of the $(N + 1)^{th}$ level.

For the case where there are 10 particles and 24 energy levels the fermi energy is 110 (in units of $\frac{\pi^2 \hbar^2}{2mL^2}$) and the maximum energy for which states are completely counted is 710. ($E_{T=0} = 110$, $\epsilon_F = 25$, $\epsilon(N + 1) = 625$). The number of energy eigenstates vs eigenenergy has been plotted like this in Figure 8. Note that unlike the bell curve that we had previously, we can show that when all states are counted, the number of available states generally rises with energy.

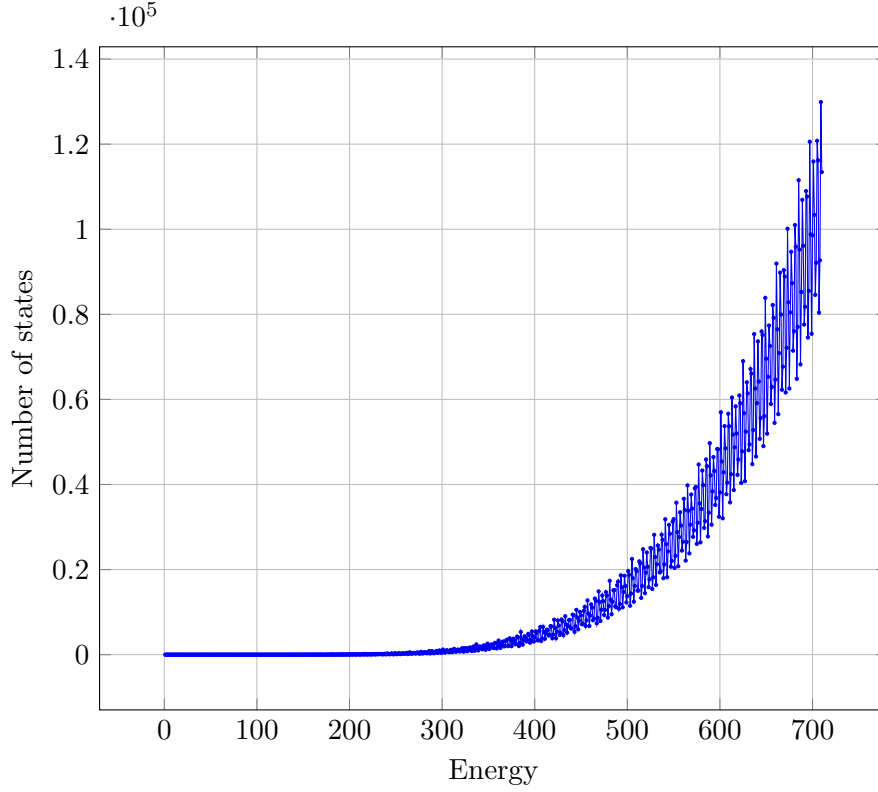


Figure 8: Number of energy eigenstates versus eigenenergy for 1 Dimensional box containing 10 identical particles. Energy is in units of $\frac{\pi^2 \hbar^2}{2mL^2}$

To calculate the partition function of the density matrix we require that the series converges before E_{max} is reached. This implicitly places an upper bound on the temperature that this model can be used for. Fig 9 shows the probability of measuring the configuration in a given energy. This distribution is calculated by computing the density operator over the basis states. ρ is plotted for different temperatures, as expected for higher temperatures the probability distribution shifts towards more energetic states. Note the discrete nature of the energies gives an extremely noisy curve. This is how the low particle regime differs drastically from statistical mechanics.

Fig 10 shows the convergence of the trace of ρ with energy. At the highest temperature the figure does not show the partition function converging; higher energies are needed to compute the final value of the partition function.

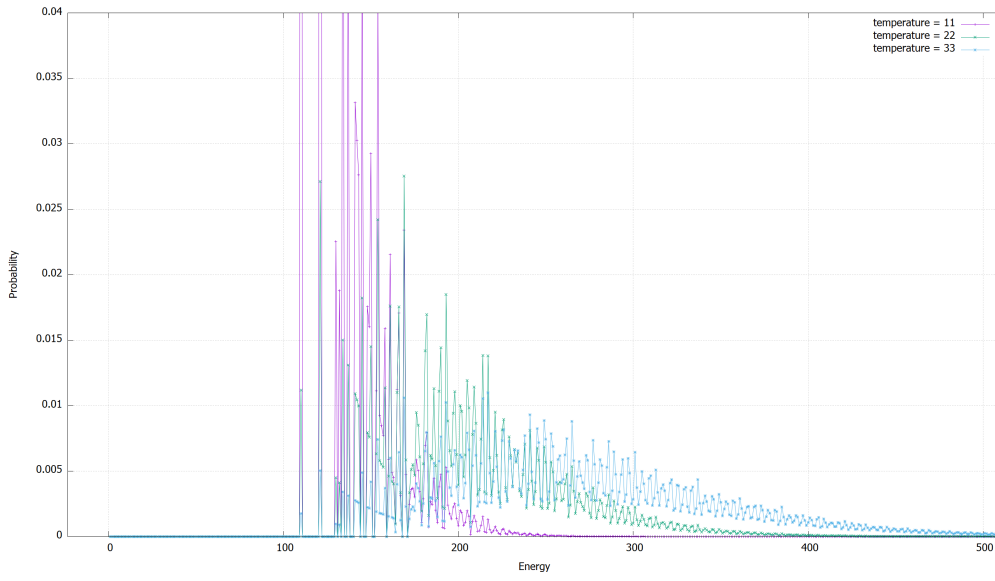


Figure 9: Density Matrix Operator. Energy is in units of $\frac{\pi^2 \hbar^2}{2mL^2}$. Temperature is in the same units as energy but divided by K_b

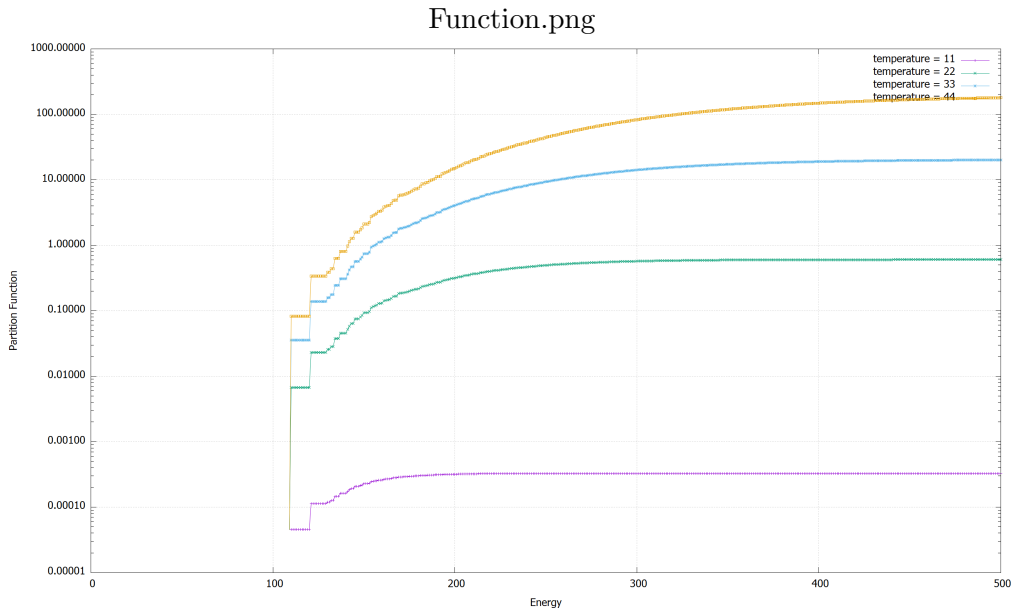


Figure 10: Convergence of the partition function. Once again Energy is in units of $\frac{\pi^2 \hbar^2}{2mL^2}$ and temperature is in the same units as energy but divided by K_b . Note the log scale of the y axis.

4.5 Recovering Fermi-Dirac Statistics

The previous graphs have shown the frequency of basis states with a given energy. Fermi-Dirac statistics describe a different parameter. They describe the average occupancy of a given energy level when the mean occupancy of all basis states have been considered. Fermi-Dirac statistics are generally quoted as a continuous function of energy, however for few particles the energy values are discrete. Here we compare energy level occupancy vs Fermi-Dirac statistics. Figures 11, ??, ??, ?? show mean occupancy as calculated from the density matrices at different temperatures. These figures have been plotted with Fermi-Dirac functions at the same temperature with a best-fit value for μ . It is clear that in the low particle count regime the mean occupancy closely approximates Fermi-Dirac statistics.

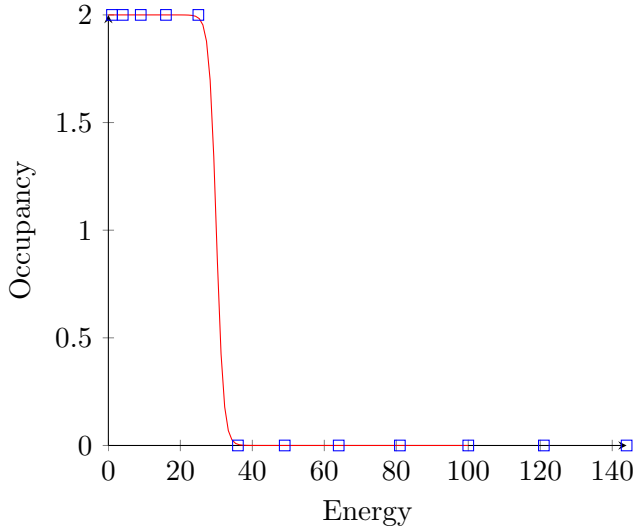


Figure 11: Mean Occupancy versus Energy in units of $\frac{\pi^2 \hbar^2}{2mL^2}$ from the density matrix and Fermi-dirac statistics at Temperature $\frac{\pi^2 \hbar^2}{2mL^2 k_B}$

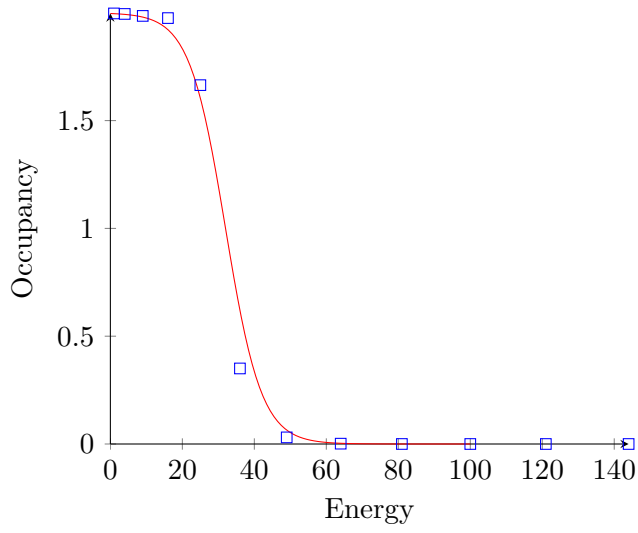


Figure 12: Mean Occupancy versus Energy in units of $\frac{\pi^2 \hbar^2}{2mL^2}$ from the density matrix and Fermi-dirac statistics at Temperature $\frac{5\pi^2 \hbar^2}{2mL^2 k_B}$

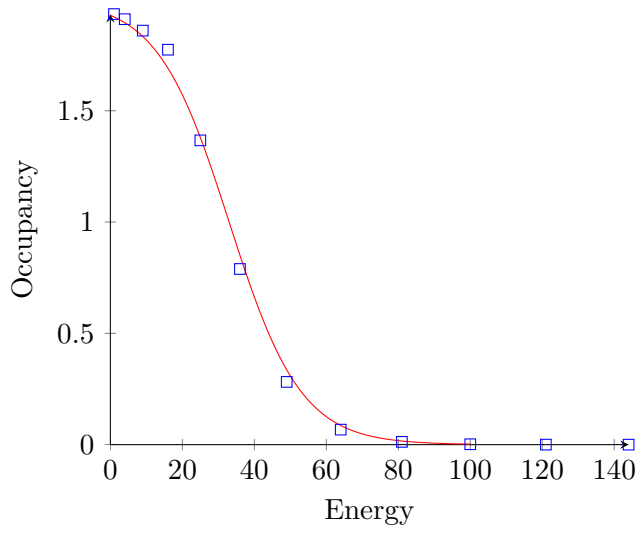


Figure 13: Mean Occupancy versus Energy in units of $\frac{\pi^2 \hbar^2}{2mL^2}$ from the density matrix and Fermi-dirac statistics at Temperature $\frac{10\pi^2 \hbar^2}{2mL^2 k_B}$

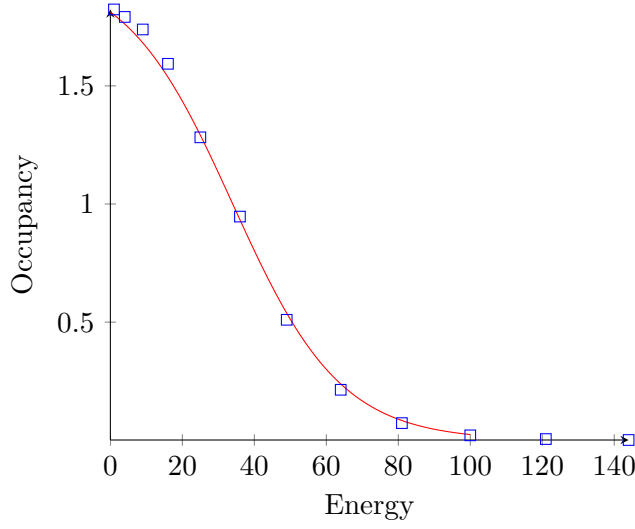


Figure 14: Mean Occupancy versus Energy in units of $\frac{\pi^2 \hbar^2}{2mL^2}$ from the density matrix and Fermi-dirac statistics at Temperature $\frac{15\pi^2 \hbar^2}{2mL^2 k_B}$

5 Calculating Thermodynamic Variables

Using equations 30 and 31 I have calculated Entropy vs Number of Particles and Temperature as well as the Total Internal Energy vs Number of Particles and Temperature.

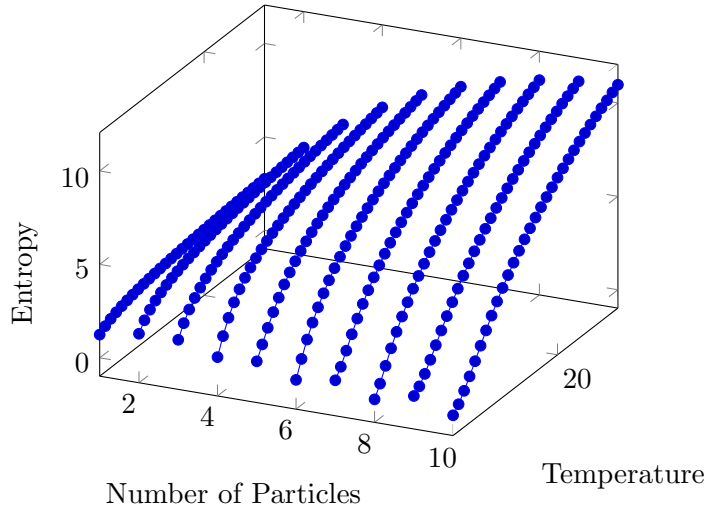


Figure 15: 3D plot of varying Number of particles to see the effects of entropy and temperature.

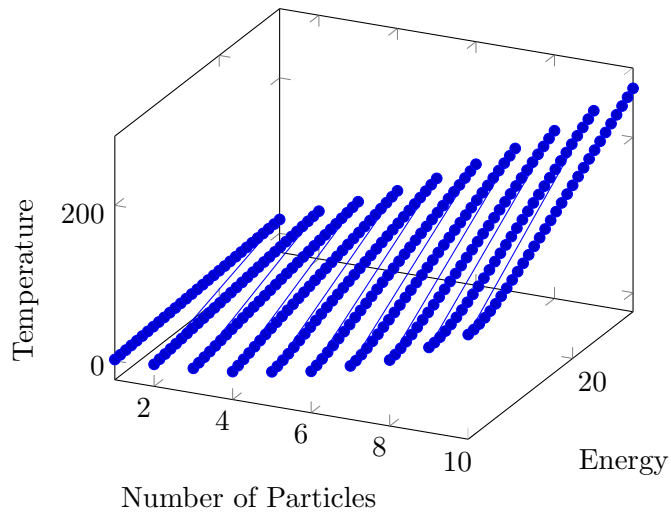


Figure 16: 3D plot of varying Number of particles to see the effects of entropy and total internal energy.

6 Quantum Szilard Engine

Here we discuss the process of inserting a partition into a 1 Dimensional box. A peculiar effect of the quantum box is that the partition insertion incurs work. The initial partition function for the system is simply $Z(L)$. After insertion of a partition at position l from left-hand side of the box (where $0 \leq l \leq L$) the new partition function is $Z(l)$. Because the number of particles in each box has not been measured $Z(l)$ is a sum over partition functions for each possibility

$$\begin{aligned} Z(l) &= \sum_{m=0}^N Z_m(l) \\ &= \sum_{m=0}^N Z_m^L(l) Z_{N-m}^R(L-l) \end{aligned}$$

where the last line shows the new partition function is a product of the two partition functions (when both contain some particles). The probability P_m of finding m particles in the left partition is given by

$$P_m = \frac{Z_m(l)}{Z(l)}. \quad (34)$$

The probabilities for finding m particles in the left-hand partition have been plotted against l .

If the variable X is varied from X_1 to X_2 isothermally, the total work in a Quantum Szilard engine [15] is

$$W = k_B T [\ln Z(X_2) - \ln Z(X_1)] \quad (35)$$

where $Z(X)$ is the partition function. Then which from above shows the work required from inserting a partition is

$$W = \left(\sum_{m=0}^N Z_m^L(l) Z_{N-m}^R(L-l) \right) - Z(L) \quad (36)$$

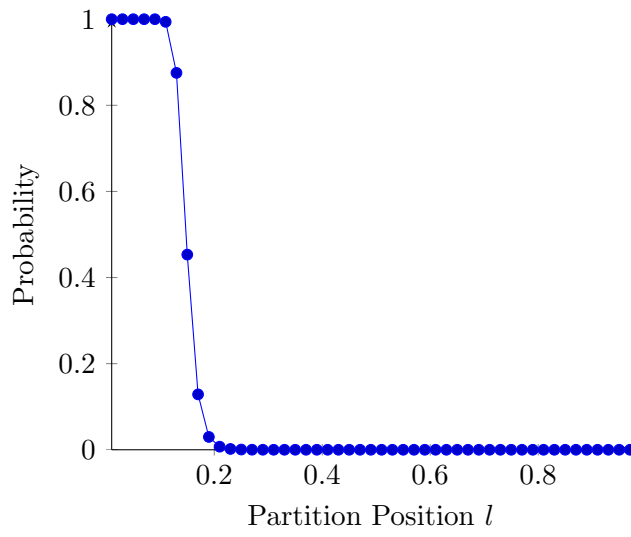


Figure 17: Probability of measuring 0 particles in the left partition versus length of left partition

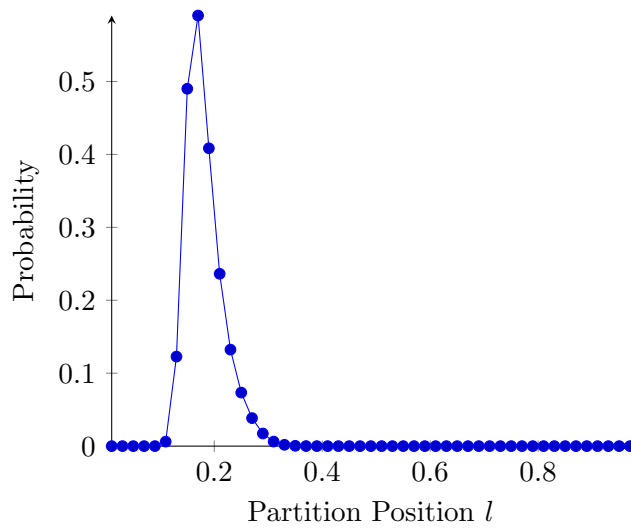


Figure 18: Probability of measuring 1 particles in the left partition versus length of left partition

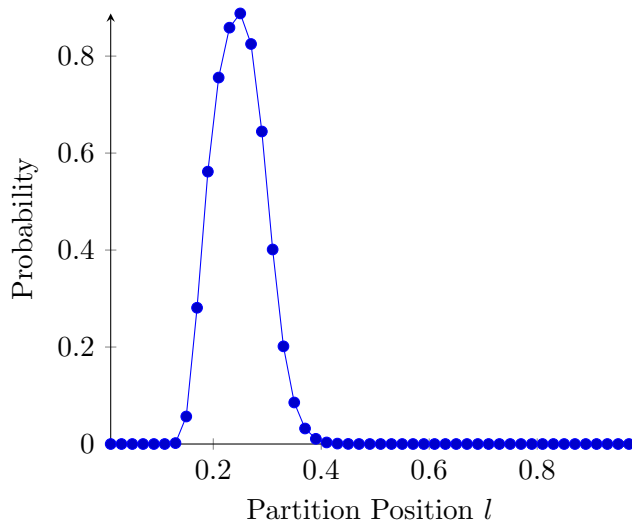


Figure 19: Probability of measuring 2 particles in the left partition versus length of left partition

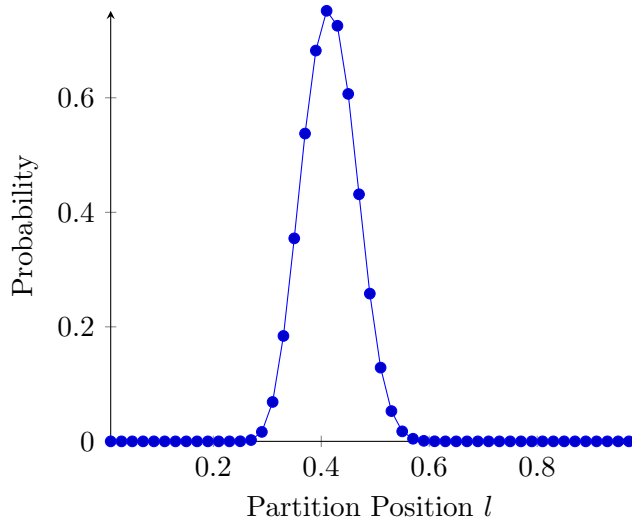


Figure 20: Probability of measuring 4 particles in the left partition versus length of left partition

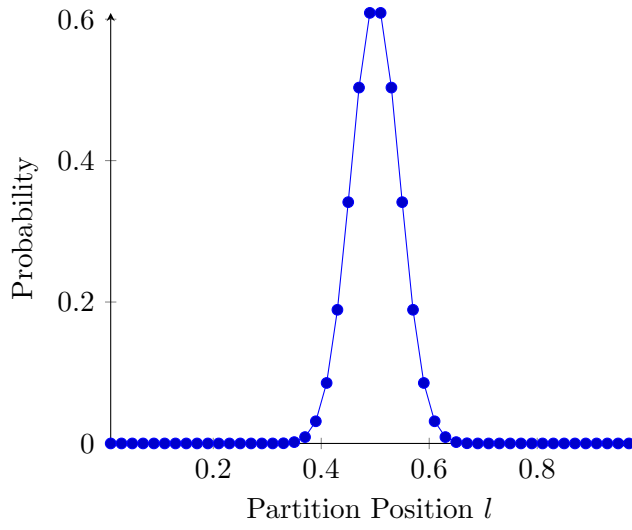


Figure 21: Probability of measuring 5 particles in the left partition versus length of left partition

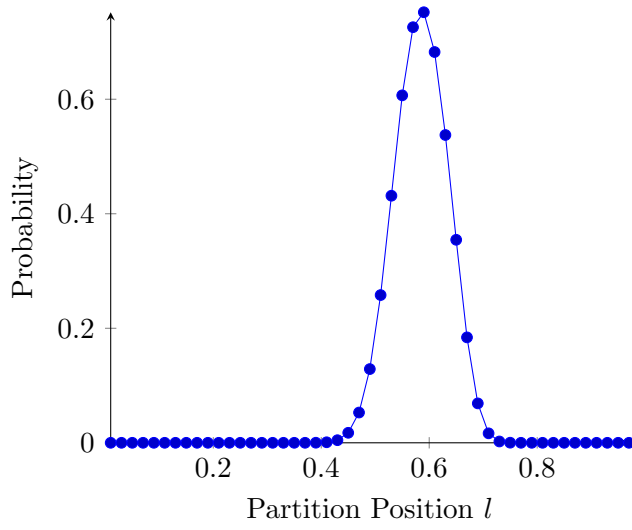


Figure 22: Probability of measuring 6 particles in the left partition versus length of left partition

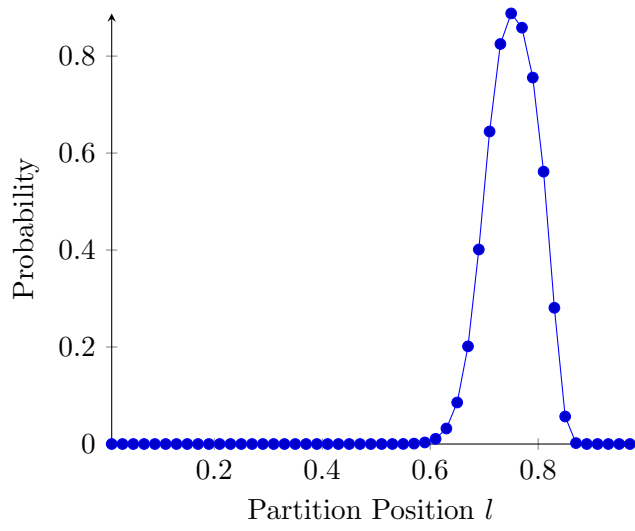


Figure 23: Probability of measuring 8 particles in the left partition versus length of left partition

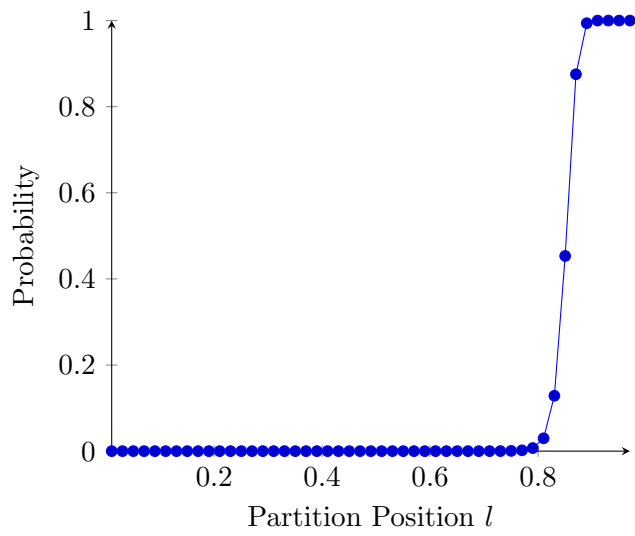


Figure 24: Probability of measuring 10 particles in the left partition versus length of left partition

7 Conclusions

In the previous work we have determined how to calculate the partition function for a 1D system containing N particles. All the thermodynamic processes of the Szilard engine involve expanding/contracting/partitioning the 1D system. The work involved in these processes is analysed by examining the partition function before and after; this is a natural extension to the work shown at the end of the previous chapter. The processes of insertion, measurement, expansion/relaxation and removal of the partition could be analysed by looking at the partition function in between each step. Throughout every single process the engine would be in contact with the thermal reservoir and every process would proceed isothermally. It can be shown then that the net work done by the engine would be greater than zero. This would show a violation of the second law at the small length scale on our well defined system. An eventual net positive work that would be computed would require Landauer's erasure principle (or equivalent) to reconcile this.

8 References

- [1] Shannon, C. (1948). A Mathematical Theory of Communication. Bell System Technical Journal, 27(4), pp.623-656
- [2] Landauer, R. (1961). Irreversibility and Heat Generation in the Computing Process. IBM Journal of Research and Development, 5(3), pp.183-191.
- [3] Plenio, M. and Vitelli, V. (2001). The physics of forgetting: Landauer's erasure principle and information theory. Contemporary Physics, 42(1), pp.25-60.
- [4] Bennett, C. (1973). Logical Reversibility of Computation. IBM Journal of Research and Development, 17(6), pp.525-532.
- [5] Norton, J. (2005). Eaters of the lotus: Landauer's principle and the return of Maxwell's demon. Studies in History and Philosophy of Science Part B: Studies in History and Philosophy of Modern Physics, 36(2), pp.375-411.
- [6] Norton, J. (2011). Waiting for Landauer. Studies in History and Philosophy of Science Part B: Studies in History and Philosophy of Modern Physics, 42(3), pp.184-198.
- [7] Kish, L. B., S. P. Khatri, C. G. Granqvist, and J. M. Smulko. "Critical Remarks on Landauer's Principle of Erasure-dissipation: Including Notes on Maxwell Demons and Szilard Engines." 2015 International Conference on Noise and Fluctuations (ICNF) (2015)
- [8] Bäuerle, A., Arakelyan, A., Petrosyan, A., Ciliberto, S., Dillenschneider, R. and Lutz, E. (2012). Experimental verification of Landauer's principle linking information and thermodynamics. Nature, 483(7388), pp.187-189.
- [9] Bäuerle, A., Petrosyan, A. and Ciliberto, S. (2015). Information and thermodynamics: experimental verification of Landauer's Erasure principle. Journal of Statistical Mechanics: Theory and Experiment, 2015(6), p.P06015.
- [10] Anders, J., Shabbir, S., Hilt, S. and Lutz, E. (2010). Landauer's principle in the quantum domain. Electronic Proceedings in Theoretical Computer Science, 26, pp.13-18.
- [11] Muschik, W., & Kaufmann, M. (1993). Quantum - Thermodynamics: Bridging Quantum Mechanics and Thermodynamics. Statistical Physics and Thermodynamics of Nonlinear Nonequilibrium Systems
- [12] L. Szilard, On the Decrease of Entropy in a Thermodynamic System by the Intervention of Intelligent Beings. Z. Phys. 53:840 (1929): English translation reprinted in Behavioral Science 9:301 (1964), as well as in Ref. 2, p. 539

- [13] Leff, H. and Rex, A. (2003). Maxwell's demon 2. Bristol: Institute of Physics Pub.
- [14] Kim, S. W., Sagawa, T., Liberato, S. D., & Ueda, M. (2011). Quantum Szilard Engine. Physical Review Letters, 106(7).